Bioorganic & Medicinal Chemistry 21 (2013) 6264–6273

Contents lists available at ScienceDirect

Bioorganic & Medicinal Chemistry

journal homepage: www.elsevier.com/locate/bmc

Identification, biological characterization and pharmacophoric analysis of a new potent and selective NK_1 receptor antagonist clinical candidate

Romano Di Fabio [*,†], Giuseppe Alvaro [‡], Simone Braggio [†], Renzo Carletti [†], Philip A. Gerrard [†], Cristiana Griffante [†], Carla Marchioro [†], Alfonso Pozzan [†], Sergio Melotto [§], Alessandro Poffe [†], Laura Piccoli [†], Emiliangelo Ratti [‖], Elvira Tranquillini [¶], Michael Trower [‖], Simone Spada [†], Mauro Corsi [†]

Neurosciences Centre of Excellence for Drug Discovery, Chemical Development and Molecular Discovery Research, GlaxoSmithKline Medicines Research Centre, Via A. Fleming 4, 37135 Verona, Italy

ARTICLE INFO

Article history:
Received 6 June 2013
Revised 29 August 2013
Accepted 1 September 2013
Available online 11 September 2013

Keywords:
Neurokinin
Substance P
G-protein coupled receptor
Central nervous system

ABSTRACT

The last two decades have provided a large weight of preclinical data implicating the neurokinin-1 receptor (NK_1) and its cognate ligand substance P (SP) in a broad range of both central and peripheral disease conditions. However, to date, only the NK_1 receptor antagonist aprepitant has been approved as a therapeutic and this is to prevent chemotherapy-induced nausea & vomiting (CINV). The belief remained that the full therapeutic potential of NK_1 receptor antagonists had yet to be realized; therefore clinical evidence that NK_1 receptor antagonists may be effective in major depression disorder, resulted in a significant further investment in discovering novel CNS penetrant druggable NK_1 receptor antagonists to address this condition. At GlaxoSmithKline after the discovery of casopitant, that went on to demonstrate efficacy as a novel antidepressant in the clinic, additional novel analogues of this NK_1 receptor antagonist were designed to further enhance its drug developability characteristics. Herein, we therefore describe the discovery process and the vivo pharmacological and pharmacokinetic profile of the new NK_1 receptor antagonist **3a** (also called orvepitant), selected as clinical candidate and further progressed into clinical studies for major depressive disorder. Moreover, molecular modeling studies enabled us to improve the pharmacophore model of the NK_1 receptor antagonists with the identification of a region able to accommodate a variety of heterocycle moieties.

© 2013 Elsevier Ltd. All rights reserved.

1. Introduction

The undecapeptide substance P (SP) is one of the most studied neurotransmitters in the CNS. Its pharmacological action is mediated by the preferential interaction with the 7-transmembrane G-coupled protein (GPCR) neurokinin 1 (NK_1) receptor. This receptor belongs to the tachykinin superfamily that consists of three receptor subtypes (NK_1, NK_2 and NK_3) and is expressed widely in the mammalian nervous system, spinal cord and peripheral tissues.[1–3] A large body of both pre-clinical and clinical evidence has linked the NK_1 receptor/SP system with a plethora of pathological conditions, ranging from pain, migraine, asthma, nausea, inflammatory bowel syndrome, cancer and urinary incontinence to anxiety and depression.[4–13]

Since the publication of the first non-peptidic NK_1 receptor antagonist in the early 1990s, there has been much effort to discover drug-like NK_1 receptor antagonists and bring them through clinical trials to the market. To date aprepitant[14] is the first and only NK_1 receptor antagonist to gain approval by the FDA; this

Abbreviations: NK, neurokinin; SP, substance P; GPCR, G protein-coupled receptor; CNS, central nervous system; SAD, social anxiety disorders; CINV, chemotherapy-induced nausea and vomiting; PoC, prove of concept; SAR, structure–activity relationship; CDI, carbonyldiimidazole; THF, tetrahydrofuran; CHO, Chinese hamster ovary; FLIPR, fluorescence imaging plate reader; GFT, gerbil foot tapping; CRC, concentration–response curve; SSRIs, selective serotonin reuptake inhibitors; HTT, human threat test; SI, social interaction; FDA, food and drug administration; i.v., intravenous; p.o., per os; Clp, clearance plasmatic.

* Corresponding author. Tel.: +39 0458218879.
E-mail address: romano.difabio@aptuit.com (R. Di Fabio).
† Present address: Aptuit S.r.l., Via A. Fleming 4, 37135 Verona, Italy.
‡ Present address: Autifony S.r.l., Via A. Fleming 4, 37135 Verona, Italy.
§ Present address: Ablicon S.r.l., Via L. Einaudi 29, 62012 Civitanova Marche (MC), Italy.
¶ Present address: Sandoz Industrial Products S.p.A., Corso Verona 165, 38068 Rovereto (TN), Italy.
‖ Present address: NeRRe Therapeutics Ltd, Gunnels Wood Road, Stevenage SG1 2FX, UK.

0968-0896/$ - see front matter © 2013 Elsevier Ltd. All rights reserved.
http://dx.doi.org/10.1016/j.bmc.2013.09.001

occurred in 2003 to control chemotherapy-induced nausea and vomiting (CINV) and, later in 2006, as a therapy for post-operative nausea and vomiting (PONV). However in the last fifteen years on the basis of initially encouraging preclinical data, several NK_1 receptor antagonists have been progressed into the clinic as potential antidepressant drugs.[15] The results from these studies have been controversial, as although efficacy in depression studies was shown initially with brain penetrant, high affinity, selective NK_1 receptor antagonists including aprepitant in their proof of concept (PoC) trials;[14,16,17] the Phase III program with aprepitant failed.[18] This led to the development of a working hypothesis that full and long lasting saturation of the central NK_1 receptor compartment is a critical requirement for the antidepressant effects of NK_1 receptor antagonists to be realized.[19] This theory was first tested in a depression clinical study with, an orally active, highly potent, selective and non-surmountable NK_1 receptor antagonist that we have previously described and termed casopitant[20] (GW679769), designated as (2*R*,4*S*)-4-(4-acetylpiperazin-1-yl)-*N*-[(1*R*)-1-[3,5-bis(trifluoromethyl)phenyl]ethyl]-2-(4-fluoro-2-methylphenyl)-*N*-methylpiperidine-1-carboxamide amine (see Figure 1). In the Phase II study casopitant delivered both a statistically and clinically significant antidepressant effect on the primary endpoint at a dose that ensured full (>99%) and sustained (24 h coverage) receptor occupancy.[19] To further improve on casopitant's profile we aimed to identify related analogues that had an enhanced metabolic stability and more favorable pharmacokinetic profile in preclinical animal species. Herein we describe the synthesis and the pharmacological and pharmacokinetic profiles of novel 4-substituted-octahydro-1*H*-pyrrolo[3,2-*c*]pyridine derivatives, shown in Figure 1. In addition, we report the results of some molecular modeling studies we performed by comparing the broad set of NK_1 receptor antagonist disclosed in literature shown in Figure 5 with the new NK_1 receptor antagonist described in this paper. This analysis confirmed that the NK_1 receptor antagonists adopt a U-shaped bioactive conformation and enabled us to identify the presence of a bulk tolerant site, able to accommodate a variety of both hydrophilic and hydrophobic moieties, as a region useful for designing novel sub-classes of NK_1 receptor antagonist analogues.

2. Materials and methods

2.1. Chemistry

The racemic bicycle γ-lactam moiety **1**, shown in Scheme 1, was synthesized as previously reported.[21,22] The resolution of the racemate was performed by preparative chiral HPLC (Chiralpack AD × 2 cm; *n*-hexane/EtOH 8:2; flux = 1 ml/min; λ = 225 nm) to afford pure enantiomers **1a** and **1b**.[23] The following reductive amination performed on the known ketone intermediate **2**,[20] with amino bicycle derivatives **1a** and **1b** in the presence of $NaBH(OAc)_3$ in dry CH_3CN, gave a mixture of epimers **3a** and **3c** and **3b** and **3d**, respectively, which were separated by flash chromatography to give title compounds.

2.2. Molecular modeling studies

NK_1 receptor antagonist structures shown in Figure 5 where used to build a common hypothesis pharmacophore applying the pharmacophore elucidate module available in the MOE software,[53] as reported in the experimental section. Then, compound **3a** was fitted into this pharmacophoric model to identify both structural similarities and differences with respect to the set of reference molecules selected in literature.

3. Discussion

Previous studies had shown that casopitant after a single oral administration in rats, was eliminated almost exclusively by loss of the *N*-acetyl group and the oxidation of the piperazine ring, leading to the cleavage of this heterocycle moiety ring.[24–26] Therefore, our design approach in preparing novel casopitant analogues was to modify the *N*-acetyl piperazine moiety of the molecule by synthesizing the corresponding more rigid bicycle γ-lactam derivative, shown in Figure 1. The four diasteroisomers **3a**, **3b**, **3c** and **3d**, as depicted in Scheme 1, obtained as described above, were characterized in the in vitro assays by increasing antagonist concentrations both in terms of receptor binding profile by displacement of [^{3}H]SP on membranes derived from CHO cells expressing the recombinant human NK_1 (hNK_1) receptor and antagonism of SP-induced release of cytosolic Ca^{2+} in hNK_1–CHO cells by using fluorometric imaging plate reader (FLIPR) technology.

As reported in Table 1, compounds **3a** and **3c** (1 pM–10 μM), exhibited the highest *in vitro* potency in the receptor binding studies at the hNK_1 receptor (pK_i = 10.20 ± 0.10 and 10.19 ± 0.13, respectively; *n* = 3 experiments). Based on these initial encouraging results, both compounds were further characterized in terms of the ability to functionally inhibit SP-induced release of cytosolic Ca^{2+} in hNK_1–CHO cells. Compounds **3a** and **3c** (0.3–10 nM), pre-incubated for 1 h at 37 °C before adding the agonist SP, as shown in Figure 2, each produced a non-surmountable antagonism of agonist CRC. For **3a** and **3c** apparent pK_B values of 10.30 ± 0.30 and 10.50 ± 0.20 (*n* = 4), respectively, were calculated by using the dose ratio of the agonist concentration response obtained in

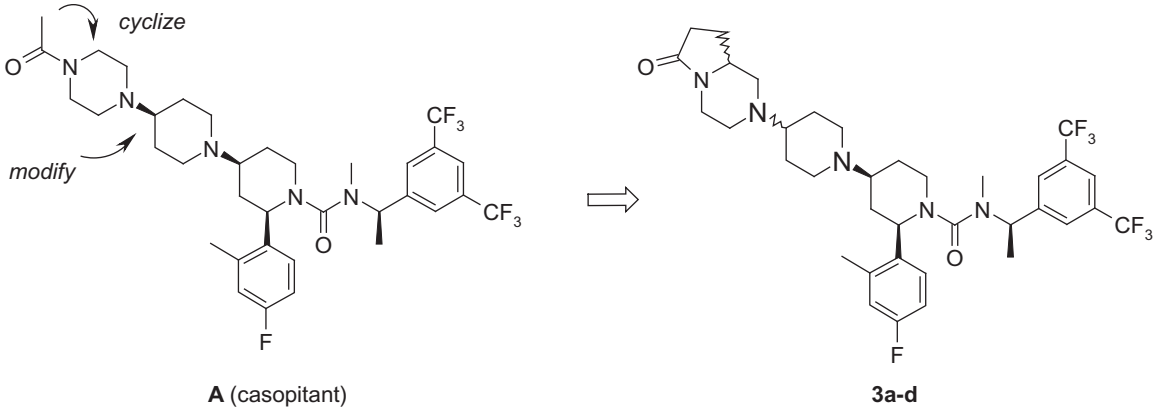

Figure 1. Modification of the piperazine moiety.

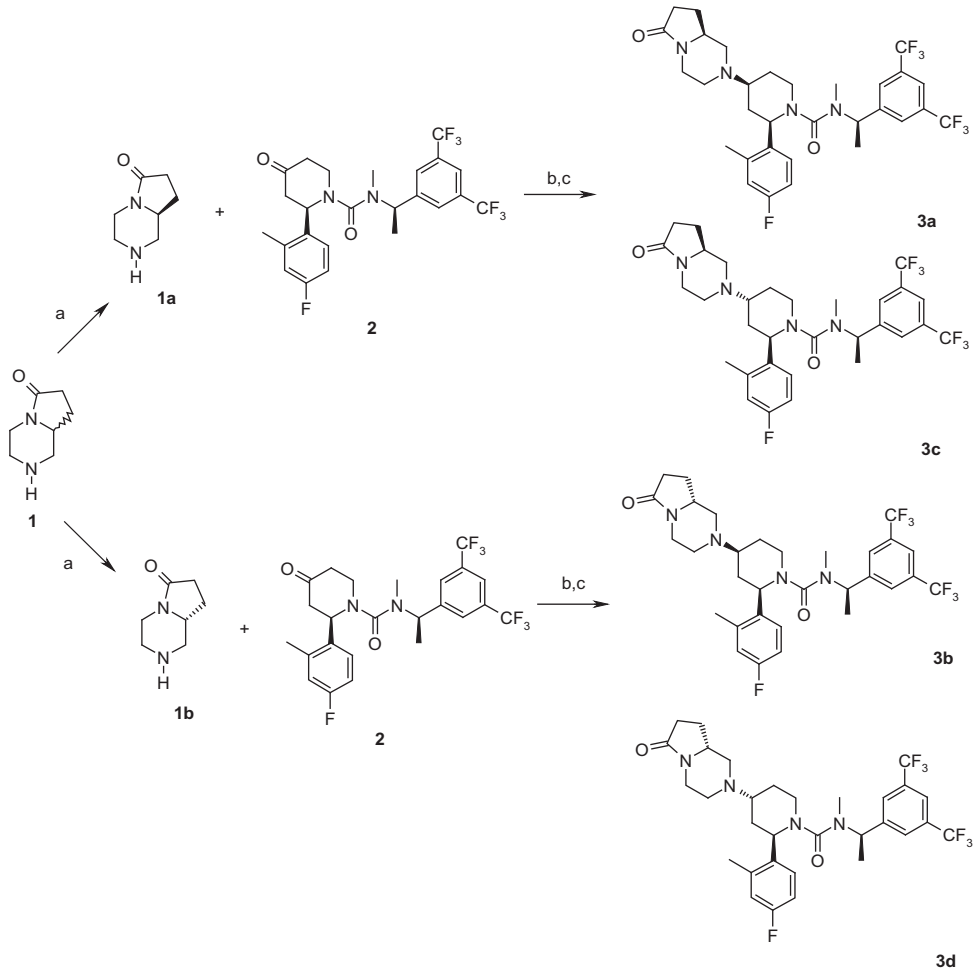

Scheme 1. (a) Chiralpack AD × 2 cm, *n*-hexane/EtOH 8:2, flux = 1 ml/min, λ = 225 nm; (b) compound **2**, dry CH_3CN, $NaBH(OAc)_3$; (c) HCl 1 M in Et_2O, 30 min, 0 °C.

Table 1
In vitro binding affinities (pK_i) and functional potencies (pK_B) at human-NK_1 receptors for NK_1 receptor antagonists

Compound	pK_i[a]	*n*	pK_B	
3a	10.20 ± 0.10	3	10.30 ± 0.30	4
3b	9.70 ± 0.04	2	NT[b]	
3c	10.19 ± 0.13	4	10.50 ± 0.20[b]	4
3d	9.86 ± 0.05	2	NT[b]	

Data are the mean ± SE of *n* experiments.
[a] pK_i and pK_B values have been determined as described in the experimental section and are the mean ± SEM of *n* experiments performed in duplicate.
[b] NT = not tested. *n* = number of experiments in duplicate.

the absence and presence of 1 nM con animal's back is turned to the observer with elevation of the tail to expose the centration of antagonist.

As reported in Table 5, compounds **3a** and **3c** exhibited good pharmacokinetics in vivo, both in rat and dog, although **3a** was more bioavailable and metabolically stable in dog than **3c**. Indeed, **3a** showed an oral bioavailability (*F*) of 17% in rat and 55% in dog, plasma clearance (Clp) of 29 ml/min/kg in rat and 6 ml/min/kg in dog and a half-life of 2.3 h in rat and 6.1 h in dog. Compound **3c** showed instead an oral bioavailability of 19% in rat and 28% in dog, a plasma clearance (Clp) of 25 ml/min/kg in rat and 11 ml/min/kg in dog and a half-life of 2.8 h in rat and 5.1 h in dog. As far as the brain penetration in rats is concerned, a *B*/*P* ratio of 1.2 and 0.9 was observed 5 min after the i.v. administration of a 1 mg/kg dose of **3a** and **3c**, respectively. Therefore both compounds **3a** and **3c** showed good pharmacokinetic properties when compared with casopitant,[20] with lower Clp, longer half-life, higher oral bioavailability and lower variability. However, compound **3a** was selected for progression over **3c** because of the more favorable prediction of the human PK profile assessed in allometric scaling studies. Compound **3a** was characterized in vivo in the gerbil foot tapping (GFT) pharmacodynamic model and later on, in the human threat test (HTT), an anxiety model in marmoset. Prior to performing these studies, receptor binding experiments were performed on homogenate derived membranes prepared from gerbil and marmoset brain cortices following the general membrane preparation protocol used with hNK_1–CHO cells, with [^{3}H]-GR205171, a highly selective radioligand for the NK_1 receptor, instead of [^{3}H]-SP, as previously described.[27] Compound **3a** (1 pM–1 μM), tested in filtration binding experiments, completely displaced [^{3}H]-GR205171 specific binding with pK_i values of 10.5 ± 0.2 (*n* = 3 experiments) on gerbil and 10.4 ± 0.1 (*n* = 4 experiments) on marmoset brain homogenates. In addition, **3a** was evaluated in terms of its pharmacokinetic profile in gerbils, showing a *B*/*P* ratio of 1.2 and a total brain concentration of 91 ng/g when administered p.o. at 1 mg/kg. The gerbil foot tapping (GFT) model is one of the preferred in vivo assay to screen NK_1 receptor antagonists.[28] This model is characterized by a typical intense foot tapping behavior induced by intracerebroventricular (icv) administration of selective NK_1 receptor agonists (e.g. GR73632).[29,30] This behavior is antagonized by CNS penetrating NK_1 receptor antagonists. In this

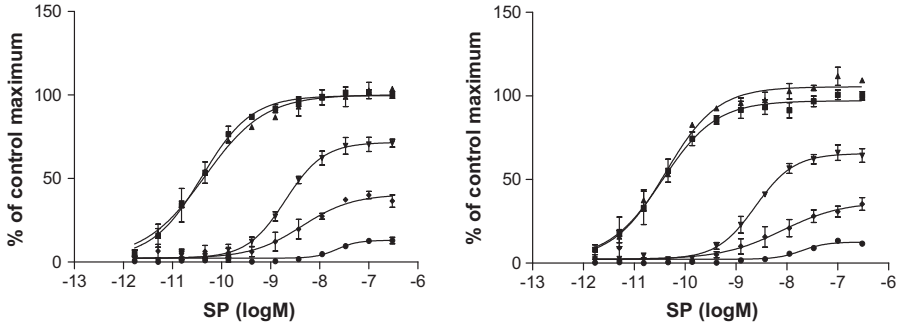

Figure 2. Increase of cytosolic calcium on hNK_1–CHO cells. Antagonism of **3a** (left) and **3c** (right) on SP-induced release of cytosolic Ca^{2+} in hNK_1–CHO. Control (■), **3a** and **3c** 0.3 nM (▲), **3a** and **3c** 1 nM (▼), **3a** and **3c** 3 nM (♦) and **3a** and **3c** 10 nM (●). Data are the mean ± SEM of four experiments performed in duplicate.

Table 2
Effect of **3a** on GFT test at different times (hours) after oral pre-treatment

Compound	−1 h	−4 h	−8 h	−24 h
3a	0.11 (0.07–0.17)	0.09 (0.06–0.13)	0.09 (0.04–0.32)	3.36 (2.60–4.40)

Data are presented as ID_{50} values (compound dose causing 50% inhibition of the tapping behavior elicited by the icv injection of GR73632, 3 pmol/5 μL) followed by 95% C.L.

model, compounds **3a** (Table 2) exhibited an excellent, dose dependent inhibition of foot tapping in gerbils after oral administration with an ID_{50} value of 0.11 mg/kg (and an ID_{50} = 0.07 mg/kg after 1hr s.c. pre-treatment) versus GR73632-induced tapping (3 pmol/5 μL). Notably, a long lasting effect was observed, the compound still being active 8 and 24 h after its oral administration (ID_{50} = 0.09 mg/kg and 3.36 mg/kg, respectively), providing evidence of the presence of compound **3a** in the brain several hours after its oral administration. Preclinical studies have reported that NK_1 receptor antagonists exhibited anxiolytic-like effects in preclinical in vivo models of anxiety.[31] Clinical evidence suggest that depression is co-morbid with anxiety in up to 60% of patients suffering for major depressive disorders. Many symptoms overlap and more than 50% of patients with generalized anxiety disorder and more than 30% of those experiencing social anxiety disorder, meet the criteria for major depressive disorders. Furthermore, SSRIs are common drugs to treat both anxiety and major depression disorders, thus suggesting that similar neurobiological alterations may occur in the two diseases. On this basis, we decided to use preclinical anxiety models, namely: human threat test in the marmoset (HTT) and social interaction (SI) in gerbils, as surrogate models to predict for potential effects of compound **3a** in major depression disorders. As far as the HTT model in marmosets is concerned, it has been suggested that the number of territorial postures elicited by marmosets, when confronted with a human observer in close proximity to the home cage, may reflect the level of stress induced in the animals.[32,33] Compound **3a** was tested at the doses of 0.3, 1, 3 and 10 mg/kg p.o. (1 h pretreatment) and, as reported in Table 3 and depicted in Figure 3, a dose dependant reduction of the number of postures was observed at 1 mg/kg (34.9% reduction vs vehicle treated animals; P <0.05), 3 mg/kg (36.6% reduction vs vehicle treated animals; P <0.05) and 10 mg/kg (46.4% reduction vs vehicle treated animals; P <0.05), suggesting a potential anxiolytic-like effect of the compound. Then, to explore whether the pharmacodynamic effect of NK_1 receptor antagonists was, as expected, dependent on their level of receptor occupancy **3a** was tested in the social interaction[34] (SI) model in gerbils and the behavioral readouts were correlated with the level of receptor engagement measured as compound receptor occupancy in gerbil striatum by using an ex vivo autoradiography method with the radioligand [^{3}H]-GR205171. Although, other models of anxiety are available in rat or mouse, their use in pre-clinical research for NK_1 receptor antagonists is complicated by species variation in

Table 3
Number of postures and their reduction (% of the reduction of the number of postures) induced by **3a** in the HTT in marmoset

Doses (po)	Number of postures	Reduction of the number of postures (%)
Vehicle	12.8 ± 2.2	—
0.3 mg/kg	11.3 ± 1.3	11.8
Vehicle	12.3 ± 1.5	—
1.0 mg/kg	8.0 ± 0.6[a]	34.9
Vehicle	11.8 ± 1.3	—
3.0 mg/kg	7.5 ± 1.3[a]	36.6
Vehicle	11.2 ± 1.3	—
10 mg/kg	6.0 ± 1.0[a]	46.4

Data are the mean ± SEM.
[a] P <0.05 compared to vehicle.

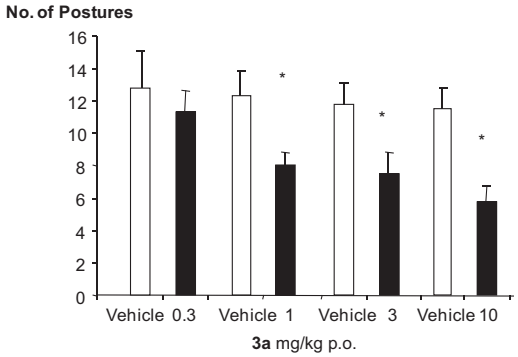

Figure 3. Number of postures and their reduction (% of the reduction of the number of postures) induced by **3a** (1 h pretreatment time) in the HTT in marmoset. Data are the mean ± SEM. *P <0.05 compared to vehicle.

Table 4
Effect of oral **3a** (1 h pretreatment time) in SI test in gerbils; data are presented as means ± SEM of 10 animals per group

Doses (po)	GSI Time (s)	% NK_1 receptor occupancy (optical density)[b]
Vehicle	21.2 ± 2.9	0% (55.3 ± 1.2)
0.1 mg/kg	22.1 ± 1.8	47.8% (28.9 ± 3.3)
0.3 mg/kg	27.383.7	74.6% (14 ± 3.6)
1.0 mg/kg	33.1 ± 3.7[a]	95.2% (2.7 ± 0.03)

[a] P <0.05 versus vehicle control. The right column reports the optical densities values of NK_1 binding as means ± SEM of 3 animals per group.
[b] Values of NK_1 receptor occupancy are expressed as percentage: see paragraph 5.2.16.

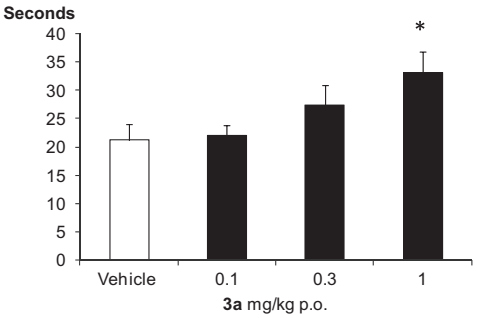

Figure 4. Effect of oral **3a** (1 h pretreatment time) in SI test in gerbils; data are presented as means ± SEM of 10 animals per group. *P <0.05 versus vehicle control.

Table 5
Preclinical pharmacokinetic parameters of compound **3a** and **3c** versus casopitant in rats and dogs[a,b]

Compound	Clp ((ml/min)/kg)	V_{ss} (l/kg)	Half-life (h)	F (%)
A (casopitant)				
(Rat)	37	3.2	1.8	8
(Dog)	10	1.9	4.5	34
3a				
(Rat)	29	3.7	2.3	17
(Dog)	6	2.0	6.1	55
3c				
(Rat)	25	3.4	2.8	19
(Dog)	11	2.0	5.1	28

[a] PK parameters derived from plasma concentrations.
[b] The PK profile was assessed at 0.5 mg/kg i.v. and 1 mg/kg p.o.

NK_1 receptor pharmacology.[27,35] Ex vivo autoradiography experiments were performed essentially as described previously.[36] **3a** was tested at the doses of 0.1, 0.3 and 1 mg/kg p.o. (1 h pre-treatment) and a dose-dependent increase of the time spent in active social interaction was observed. A significant increase in seconds (s) was recorded at 1 mg/kg (21.2 ± 2.9 s in vehicle to 33.1 ± 3.7 s after treatment, P <0.05). No effect was observed on animals' locomotor activity, thus excluding any sedative effect induced by the compound (Table 4 and Figure 4). NK_1 receptor occupancy in the gerbil striatum at the effective dose of **3a** (1 mg/kg) in the SI test was 95.2% whereas the non-effective doses of 0.3 and 0.1 mg/kg produced levels of NK_1 receptor occupancy of 74.6% and 47.8%, respectively (Table 4). These results confirm that high levels (>90%) of NK_1 receptor occupancy are necessary to elicit a significant pharmacodynamic effect in the SI model in gerbils.

Finally the in vitro receptogram screen (by MDS Pharma Service, Taiwan) confirmed that **3a** is highly selective for the hNK_1 receptor since at 10 μM concentration it produced less than 50% displacement of binding in the full battery of 67 receptors, transporters, ion channels and enzymes with exception of the following targets: sigma σ1, platelet activating factor, sigma σ2, sodium channel (site 2) for which the following pK_i values were estimated: sigma σ1 (K_i = 0.94 μM), platelet activating factor (K_i = 2.27 μM), sigma σ2 (K_i = 3.26 μM), sodium channel (K_i = 4.54 μM). In light of the subnanomolar affinity shown for **3a** at human NK_1 receptor (pK_i = 10.2; K_i = 0.06 nM), it is estimated that the selectivity for hNK_1 receptor over all the receptors screened by MDS Pharma Services is at least 10,000-fold.

Molecular modeling studies were performed on compound **3a** which was fitted into a pharmacophoric model created from the set of known NK_1 receptor antagonists, showed in Figure 5, with the aim to identify both structural similarities and/or differences amongst compound **3a** and the reference compounds. In a previous pharmacophore model hypothesis for NK_1 receptor antagonists,[2,28,37–40] the presence of two distal aryl groups, undertaking a Π-stacking interaction, is considered critical to enable NK_1 receptor antagonists to adopt a U-shaped bioactive conformation.[41] Other authors reported the presence of an edge-Π interaction between similar aryl moieties.[42] Then, NMR studies on tripepdides NK_1 receptor antagonists confirmed that two distal aromatic rings are stacked each other.[43] In Figure 6 is reported the superimposition of compound **3a** and the set of NK_1 receptor antagonists shown in Figure 5. These compounds share at least four pharmacophoric features, namely: two distal aryl rings, an H-bond acceptor group, present in the right hand side chain, and a heterocycle core bearing an amine or amide function. The presence of the two distal aromatic rings at the appropriate distance and correctly oriented within the chemical space, confirm the hypothesis of the NK_1

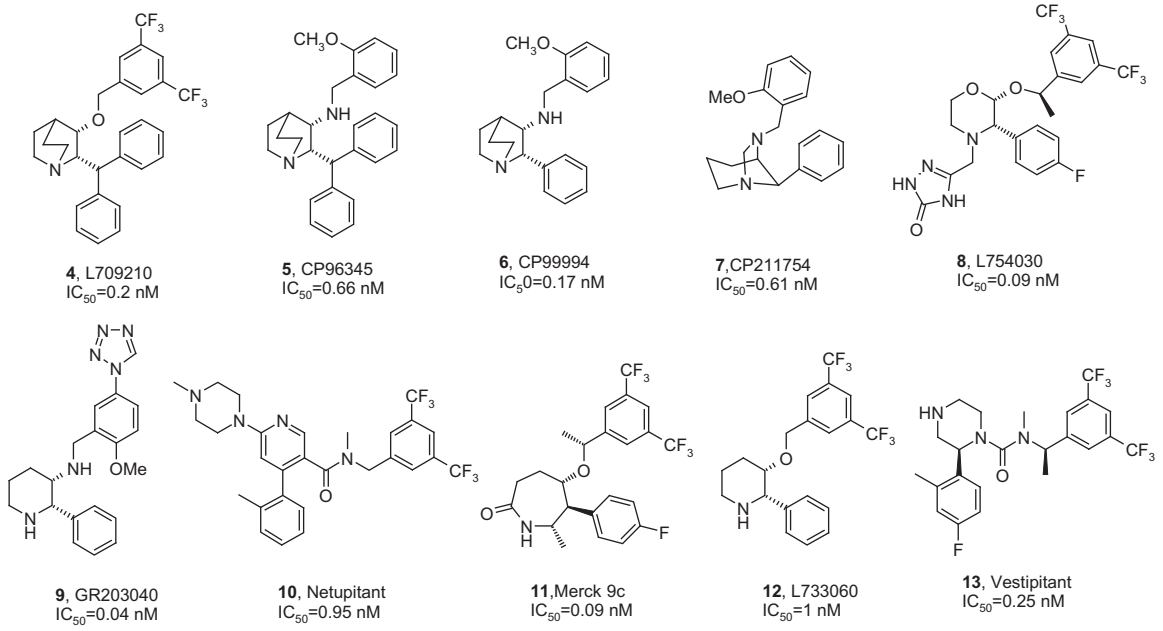

Figure 5. Chemical structure and in vitro activity of the set of NK_1 receptor antagonists used to build a common features pharmacophore model.

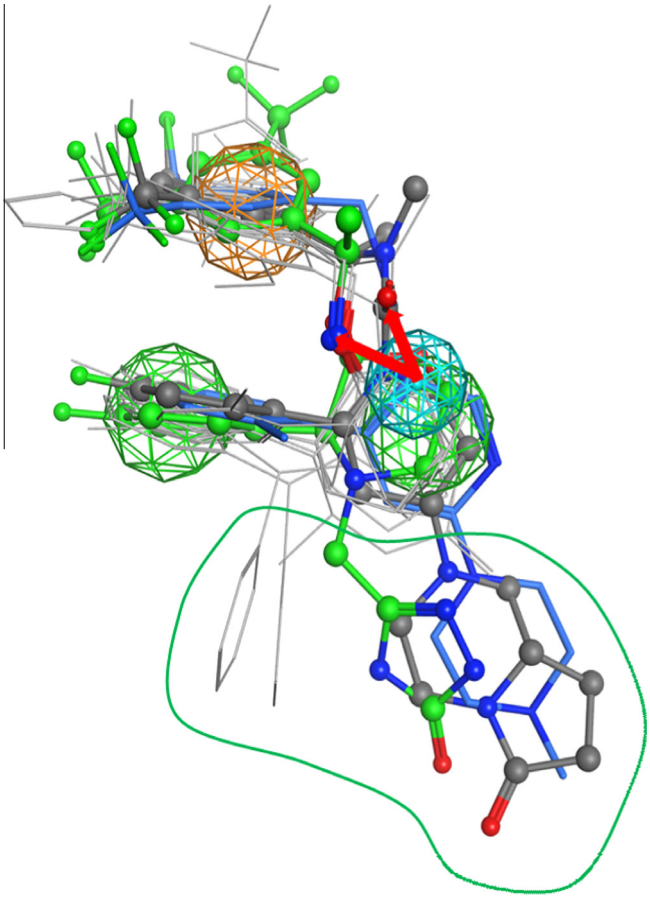

Figure 6. Superimposition of the set of NK_1 receptor antagonists **4**–**13** selected in literature, shown in Figure 5, and compound **3a** and identification of four distinct pharmacophoric features, namely: two hydrophobic regions (green) one aromatic point (orange) and one hydrogen bond acceptor (cyano). The two red arrows indicate the hydrogen bonds vectors projected from the putative hydrogen bond donor represented by the cyano sphere. The green contoured area represents a region of the space in which different hydrophilic (heterocycle rings) and hydrophobic (phenyl rings) moieties are tolerated.

receptor antagonists adopt a U-shaped (stacked or slightly displaced) bioactive conformation. In addition, despite the significant structural difference existing between compound **3a** and aprepitant, both in terms of heterocycle core and scaffold decoration, these NK_1 receptor antagonists seem to share the same pharmacophoric features. In particular, it is worth noting that the hydrophilic moieties, namely the bicycle γ-lactam and the triazolidinone present in the north-western and south-western region of these compounds, respectively, occupy the same binding site region, enabling the relative carbonyl groups to act as H-bond acceptors. In summary, this analysis shown that compound **3a** shares the same U-shaped bioactive conformation hypothesized in the past for other structural diverse series of NK_1 receptor antagonist; in addition this study enabled to identify an accessory bulk tolerant site, able to accommodate a variety of both hydrophilic and hydrophobic moieties, as a useful region to design novel sub-series of NK_1 receptor antagonists and/or optimizing their physicochemical and pharmacokinetic properties.

4. Conclusion

In summary, compound **3a** is a new in vitro and in vivo potent highly brain penetrating NK_1 receptor antagonist, showing long lasting pharmacological activity in the gerbil foot tapping test (up to 24 h), and anxiolytic-like properties both in the human threat test in marmoset and in the social interaction model in gerbils. In the latter test a full NK_1 receptor occupancy was observed to be needed to produce a significant pharmacodynamic effect. Compared to casopitant, due to its purposefully engineered more rigid bicycle γ-lactam structure, compound **3a** showed an improved preclinical pharmacokinetic profile. Based upon its favorable pharmacokinetics and developability profile **3a** (termed orvepitant) was selected as a drug candidate and has been progressed to clinical studies. The outcome of these studies, including in patients suffering from major depressive disorder, is reported elsewhere.[44]

5. Experimental

5.1. Chemistry

NMR spectra were recorded in DMSO-d_6 or $CDCl_3$ at constant temperature of 25 °C and complete assignment were made by means of several 1D and 2D-techniques including ^{19}F, *g*COSY, *g*HSQC, *g*HMQC NMR-experiments when needed. ^1H and *g*HSQC experiments were collected on a 400 Unity Varian or 500 *Inova* Varian. Chemical shifts are reported in parts per million (ppm) downfield from $CHCl_3$ residual line (δ = 7.27 ppm) or from DMSO residual line (δ = 2.49 ppm) and were assigned as singlets (s), doublets (d), triplets (t), quartet (q), broad quartet (bq), broad singlets (bs), doublets of doublets (dd), or multiplets (m). Coupling constants (*J*) are given in Hz. IR spectra were recorded on a Nicolet Magna 760 (Thermo Fisher Scientific) spectrometer. Mass spectra analyses were performed on a VG Platform (Waters, Manchester, UK), mass spectrometer operating in positive electrospray ion mode. Analytical thin layer chromatography (t.l.c.) was performed on glass plates (Merck Kieselgel 60 F254). Visualization was accomplished by UV light (254 nm), I_2. Column chromatography was performed on silica gel (Merck Kieselgel 70–230 mesh). Chemical purity of compounds has been assessed by HPLC (>95%). All reactions were carried out under anhydrous N_2 atmosphere using standard Schlenk techniques. Most chemicals and solvents were analytical grade and used without further purification.

5.1.1. General procedure for the preparation of compounds 3a, 3b, 3c, 3d

A solution of intermediate **2** (2.4 g, 5 mmoles) in 80 ml of dry CH_3CN was added to a solution of intermediate **1a** or **1b** (5.7 g, 40.7 mmol) dissolved in 30 ml of dry CH_3CN under nitrogen atmosphere at room temperature. Sodium triacetoxyborohydride (4.36 g, 20.6 mmol) was added portionwise at room temperature over 1 h min. The reaction mixture was stirred at room temperature for 22 h. Then 75 ml of H_2O and 25 mL of a saturated solution of $NaHCO_3$ were added and the solution was extracted with AcOEt (2 × 200 ml). The organic layers were collected and dried over dry Na_2SO_4, filtered and evaporated in vacuo. The crude residue was purified by flash chromatography (silica gel, AcOEt/CH_3OH 9:1) to give title diasteroisomers **3a** and **3c** from intermediate **1a**, and **3b** and **3d** from intermediate **1b**. Then, the solution of the single diasteroisomers **3a**, **3b**, **3c** and **3d** in dry Et_2O, was treated with 1.5 equiv of HCl (1 M in Et_2O). The solution was stirred for 30 min at 0 °C, evaporated in vacuo and the solid residue was washed with n-pentane to afford title hydrochloride derivatives as white solids.

5.1.2. (2*R*,4*S*)-4-[(8a*S*)-6-Oxo-octahydropyrrolo[1,2-a]piperazin-2-yl]-*N*-[(1*R*)-1-[3,5-bis(trifluoromethyl)phenyl]ethyl]-2-(4-fluoro-2-methylphenyl)-*N*-methylpiperidine-1-carboxamide hydrochloride (3a)

^1H NMR (DMSO-d_6): δ (ppm) 10.22 (br s, 1H); 7.99 (s, 1H); 7.67 (s, 2H); 7.22 (dd, 1H); 6.94 (dd, 1H); 6.81 (t, 1H); 5.31 (q, 1H); 4.20 (dd, 1H); 4.00–3.86 (br m, 2H); 3.60–3.40 (m, 2H); 3.1–2.7 (m, 4H);

2.73 (s, 3H); 2.40–2.00 (m, 5H); 2.35 (s, 3H); 1.94 (m, 1H); 1.74 (q, 1H); 1.57 (d, 3H); 1.46 (d, 3H).

MS (ES/+) m/z = 629 $[M+H]^+$.

HPLC: supercolis ABZ plus column (25 cm × 4.6 mm × 5 μ); mobile phase NH4OAc 10 mM/CH_3CN from 60:40 to 10:90 in 5 min, then NH4OAc 10 mM/CH_3CN 10:90 for 10 min; flux: 0.8 ml/min; λ = 220 nm; retention time = 9.27 min.

5.1.3. (2*R*,4*S*)-4-[(8a*R*)-6-Oxo-octahydropyrrolo[1,2-*a*]piperazin-2-yl]-*N*-[(1*R*)-1-[3,5-bis(trifluoromethyl)phenyl]ethyl]-2-(4-fluoro-2-methylphenyl)-*N*-methylpiperidine-1-carboxamide hydrochloride (3b)

^{1}H NMR (DMSO-d_6): δ (ppm) 11.05 (br s, 1H); 7.95 (s, 1H); 7.64 (s, 2H); 7.19 (dt, 1H); 6.90 (dd, 1H); 6.78 (dt, 1H); 5.28 (q, 1H); 4.16 (dd, 1H); 3.53 (m, 2H); 3.41 (m, 2H); 3.17 (t, 1H); 2.94 (m, 2H); 2.96–2.80 (m, 2H); 2.75 (t, 1H); 2.69 (s, 3H); 2.30–2.00 (m, 1H); 1.90 (m, 1H); 1.75 (q, 1H); 1.50 (m, 1H); 1.43 (d, 3H).

MS (ES/+) m/z = 629 $[M+H]^+$.

HPLC: supercolis ABZ plus column (25 cm × 4.6 mm × 5 μ); mobile phase NH4OAc 10 mM/CH_3CN from 60:40 to 10:90 in 5 min, then NH4OAc 10 mM/CH_3CN 10:90 for 10 min; flux: 0.8 ml/min; λ = 220 nm; retention time = 8.86 min.

5.1.4. (2*R*,4*R*)-4-[(8a*S*)-6-Oxo-octahydropyrrolo[1,2-a]piperazin-2-yl]-*N*-[(1*R*)-1-[3,5-bis(trifluoromethyl)phenyl]ethyl]-2-(4-fluoro-2-methylphenyl)-*N*-methylpiperidine-1-carboxamide hydrochloride (3c)

^{1}H NMR (DMSO-d_6): δ (ppm) 10.65 (br m, 1H); 7.99 (s, 1H); 7.76 (s, 2H); 7.37 (dd, 1H); 7.01 (dd, 1H); 6.93 (dd, 1H); 5.24 (br m, 1H); 5.04 (q, 1H); 4.00–3.95 (br m, 2H); 3.68 (m, 1H); 3.58 (m, 2H); 3.51 (m, 1H); 3.24–3.15 (m, 2H); 2.96 (m, 1H); 2.85 (m, 1H); 2.54 (m, 3H); 2.36–2.13 (m, 6H); 2.21 (s, 3H); 1.72 (m, 1H); 1.59 (m, 1H); 1.57 (d, 3H).

MS (ES/+) m/z = 629 $[M+H]^+$.

HPLC: supercolis ABZ plus column (25 cm × 4.6 mm × 5 μ); mobile phase: NH4OAc 10 mM/CH_3CN from 60:40 to 10:90 in 5 min, then NH4OAc 10 mM/CH_3CN 10:90 for 10 min; flux: 0.8 ml/min; λ = 220 nm; retention time = 8.84 min.

5.1.5. (2*R*,4*R*)-4-[(8a*R*)-6-Oxo-octahydropyrrolo[1,2-a]piperazin-2-yl]-*N*-[(1*R*)-1-[3,5-bis(trifluoromethyl)phenyl]ethyl]-2-(4-fluoro-2-methylphenyl)-N-methylpiperidine-1-carboxamide hydrochloride (3d)

^{1}H NMR (DMSO-d_6): δ (ppm) 10.90–10.60 (br m, 1H); 7.99 (s, 1H); 7.76 (s, 2H); 7.36 (dt, 1H); 7.00 (dd, 1H); 6.92 (dt, 1H); 5.25 (br t, 1H); 5.05 (q, 1H); 3.98 (m, 2H); 3.67 (m, 2H); 3.58 (m, 1H); 3.44 (m, 1H); 3.20 (m, 2H); 2.90 (m, 2H); 2.53 (s, 3H); 2.22 (s, 3H); 2.40–2.10 (m, 6H); 1.73 (m, 1H); 1.56 (m, 1H); 1.57 (d, 3H).

MS (ES/+) m/z = 629 $[M+H]^+$.

HPLC: supercolis ABZ plus column (25 cm × 4.6 mm × 5 μ); mobile phase NH4OAc 10 mM/CH_3CN from 60:40 to 10:90 in 5 min, then NH_4OAc 10 mM/CH_3CN 10:90 for 10 min; flux: 0.8 ml/min; λ = 220 nm; retention time = 9.28 min.

5.2. Biology

5.2.1. Membrane preparation from hNK$_1$–CHO cells

CHO cells expressing hNK$_1$ receptors[45] were cultured in Ham's F-12 medium supplemented with 10% (v/v) heat-inactivated foetal bovine serum, 2 mM glutamine and 0.2 mg/ml G 418.

Membrane preparation from hNK$_1$–CHO cells was performed essentially as described by Beattie et al. (1995).[46] When confluent, hNK$_1$–CHO cells were harvested in phosphate buffered saline (PBS) containing 5 mM EDTA and centrifuged at 913*g* for 8 min at 4 °C. Cells were then resuspended in 10 volumes of HEPES (50 mM) buffer (pH 7.4), containing leupeptin (0.1 mM), bacitracin (40 μg/ml), EDTA (1 mM), Pefabloc (1 mM) and pepstatin A (2 μM) and homogenized using a Polytron. The suspension was centrifuged at 48,000*g* for 20 min at 4 °C. The final pellet was resuspended in 10 volumes of membrane preparation buffer and re-homogenized. Suspensions of membrane were then frozen at −80 °C until required. Protein concentration was determined by the Bio-Rad Protein assay using bovine serum albumin (BSA) as the standard.

5.2.2. Preparation of brain homogenates from gerbil and marmoset

Mongolian gerbil (60 g, Charles River) and common marmoset (300–400 g, GSK colony, Verona, Italy) homogenates obtained from cerebral cortex and striatum (gerbil) and cerebral striatum (marmoset) were prepared as follows. Fresh tissues were weighed, crumbled and homogenized in 10 volumes of membrane-preparation buffer (HEPES 50 mM pH 7.4, leupeptin 0.1 mM, bacitracin 40 μg/ml, EDTA 1 mM, Pefabloc 0.2 mM, pepstatin 2 μM). The homogenate was then centrifuged at 48,000*g* for 20 min, and the pellet was washed once more by resuspension in 10 volumes of membrane preparation buffer and centrifugation at 48,000*g* for 20 min. The final pellet was resuspended in 7–10 volumes of membrane preparation buffer and subdivided in aliquots frozen at −80 °C until use. Protein concentration was determined by the Bio-Rad Protein assay using bovine serum albumin (BSA) as the standard.

5.2.3. [^{3}H]-SP binding on membranes from hNK$_1$–CHO cells

Binding assays were carried out in 96 well, flat bottom, plates (Sarstedt). The assay volume of 200 μl consisted of 2 μl of DMSO or increasing concentrations of test compound dissolved in DMSO (1 pM–1 μM final concentration), 100 μl of [^{3}H]-SP, (0.5 nM final concentration), and 100 μl of membrane suspension (8 μg of protein per well) in incubation buffer (containing 50 mM HEPES, pH 7.4, 3 mM $MnCl_2$, and 0.02% BSA).

In saturation experiments, increasing concentrations of [^{3}H]-SP (1 pM–3 nM) were incubated as above. Non specific binding was defined by the addition of 1 μM SP. The incubation was carried out at room temperature for 40 min. Non-specific binding was defined by the addition of cold SP (1 μM). The reaction was stopped by rapid filtration through GF/B filterplates pre-soaked in 0.5% polyethylenimine (PEI) using a Packard cell harvester. Filters were washed 5 times with 200 μl of ice-cold 0.9% w/v NaCl, and radioactivity was counted in a microplate scintillation counter (Top Count, Packard). In each experiment, every concentration of displacer was tested in duplicate.

5.2.4. [^{3}H]-GR205171 binding on cerebral tissues from gerbil and marmoset

Binding assays were carried out in 96 deep well polypropylene plates (Whatman). In displacement experiments, the assay volume of 400 μl consisted of 100 μl of incubation buffer (containing 50 mM HEPES, pH 7.4, 3 mM $MnCl_2$, and 0.02% BSA), 4 μl of DMSO or increasing concentrations of test compound dissolved in DMSO (1 pM–1 μM final concentration), 100 μl of [^{3}H]-GR205171 (0.2 nM final concentration) in incubation buffer and 200 μl of membrane suspension containing 0.055 mg (gerbil) or 0.080 mg (marmoset) protein dissolved in incubation buffer with the addition of 2 μg/ml leupeptin, 20 μg/ml Bacitracin and 0.5 μM phosphoramidon. In saturation experiments, increasing concentrations of [^{3}H]-GR205171 (1 pM–3 nM) were incubated as above. Non specific binding was defined by the addition of 1 μM GR205171. The incubation proceeded at room temperature for 60 min. Non-specific binding was defined by the addition of cold GR205171 (1 μM).

The reaction was stopped by rapid filtration through GF/C filtermats pre-soaked in 0.5% polyethyleneimine (PEI) using a Brandel M/96R cell harvester. Filters were washed 3 times with 1 ml ice cold wash buffer (containing 50 mM HEPES, pH 7.4, and 3 mM $MnCl_2$), and radioactivity was counted in a liquid scintillation counter (Beta Counter, Packard). In each experiment, every concentration of displacer was tested in duplicate.

5.2.5. Measurement of $[Ca^{2+}]_i$ using FLIPR in hNK_1–CHO cells

hNK_1–CHO cells were seeded into black walled clear-bottom 96-well plates (Costar, UK) at a density of 60,000 cells per well and cultured overnight. The cells were then incubated for the labelling in the culture medium containing the fluorescent calcium indicator Fluo-4 AM (2 μM), the organic anion transport blocker probenecid (5 mM), and HEPES (20 mM) for 30 min in a humidified atmosphere of 5% CO_2. After washing with Hanks' Balanced Salts Solution (HBSS) containing 20 mM HEPES and 2.5 mM probenecid (wash buffer), the cells were incubated for 60 min at 37 °C in wash buffer containing 0.02%BSA (assay buffer) either in the absence (control) or in the presence of test compound (0.3–10nM). The plates were then placed into a FLIPR (Molecular Devices, Sunnyvale, CA) to monitor cell fluorescence (λ_{ex} = 488 nm, λ_{em} = 510–570 nm) before and after the addition of different concentrations of SP (2 pM–300 nM) in assay buffer. FLIPR experiments were carried out by using a laser setting of 1.0 W and a 0.4 sec CCD (charge coupled device) camera shutter speed. In each experiment, the test compound was tested in duplicate versus every concentration of SP.

5.2.6. Drugs and materials for in vitro studies

Each test compound was freshly prepared in each experiment as 100 μM solution in DMSO diluted from a 10 mM stock solution in DMSO. All further dilutions were performed in either DMSO in the binding experiments or in the assay buffer in the functional experiments. [^{3}H]-SP (1–2 TBq/mmol) was purchased from Amersham Life Science. [^{3}H]-GR205171, di-trifluoroacetic acid salt, synthesised in GSK Chemical Department and labelled with [^{3}H] by Amersham, has been provided as 3.07 TBq/mmol, in ethanol solution. SP was obtained from Bachem. Fluo-4 was purchased from Molecular Probes. G-418 was purchased from Calbiochem. Probenecid was purchased from Sigma–Aldrich. Leupeptin, bacitracin, Pefabloc, pepstatin A, phosphoramidon were purchased from Sigma–Aldrich. FLIPR was purchased from Molecular Devices (Sunnyvale, CA).

5.2.7. Data analysis for receptor binding and functional studies

Data from competition binding experiments on membranes from hNK_1–CHO cells were analyzed by using the non-linear curve-fitting program MicroSAT 5.2.1. For [^{3}H]-SP displacement binding experiments, IC_{50} values were obtained constraining the slope factor to unity. IC_{50} values were converted to K_i using the Cheng–Prusoff equation.[47] Data from competition binding experiments on brain homogenates were analyzed using the non-linear curve-fitting program LIGAND.[48] Previous determination of K_D of radioligands was assessed by elaborating saturation experiments with LIGAND. In FLIPR experiments on hNK_1–CHO cells, functional responses were measured as fluorescence intensity (FI) produced after receptor stimulation minus basal FI. Curve fitting was determined by non-linear regression analysis using GraphPad prism Version 3.02. In functional experiments, the apparent pK_B value for **3a** and **3c** were calculated by using the Gaddum equation: $pK_B = \log(\text{concd ratio} - 1) - \log(\text{antag concd})$, where concd ratio represents the ratio between the EC_{50} values of the agonist in the presence and in absence of the antagonist.

5.2.8. Gerbil foot tapping (GFT)

The subjects were male Mongolian Gerbils (50–70 g) obtained from the Charles River colony (Italy). Animals were housed in groups of 5 under standard laboratory conditions (23 ± 1 °C; light on 0600–1800 h). Animals were moved from the housing room to the experimental room one hour prior to the start of the experiment. Gerbils were briefly anaesthetised by inhalation of an isoflurane/oxygen mixture (3% v/v). The skull was exposed and 5 μl of GR73632 (3 pmol/5 μl) injected directly into the lateral ventricle by the insertion of a cuffed 25 gauge needle to a depth of 4 mm below bregma. Immediately after treatment the animals were placed individually into clear Perspex observation boxes containing a layer of sawdust. Following recovery, the duration of repetitive hind foot tapping was recorded for 3 min, giving a maximum possible duration of 180 sec.

5.2.9. Human threat test (HTT) in marmoset

The studies utilised laboratory-bred male (vasectomised) and female common marmosets over 2 years of age, weighing 300–500 g. The animals were caged in couples, in a housing room maintained at 25 ± 1 °C, 60% humidity and a 12 h light/dark cycle (lights on at 0600, with 30 min simulated dawn and twilight). Both animals in each pair were involved in the test, which was carried out with the animals situated in the home cage. Because there are great differences in behavior between subjects, the 'responder' animals included in an anxiety study were preselected and had to meet the baseline criteria of at least 10 postures exhibited in the 2 min of test period.

The postures recorded in the test were those described by Costall et al. (1988).[32]

- *Genital presenting* (*'Tail Posture'*): the animal's back is turned to the observer with elevation of the tail to expose the genital region;
- *Scent-marking*: the animal scent-marks the cage surfaces using circum-anal and circum-genital scent glands;
- *Slit-stare*: the animal stares at the observer with flattened ear tufts and eyes reduced to 'slits'
- *Arch-piloerection*: the animal moves around the cage with arched back and full-body piloerection, failing to make eye contact with the observer.[24]

The number of jumps from the back of the cage to the cage front provided an index of locomotor activity.

5.2.10. GFT experimental design

1, 4, 8 or 24 h before the GR73632 administration, at least 7 animals received each treatment of vehicle or test compound (10 ml/kg). All treatments were randomly distributed between the five animals of each cage. On completion of experiments animals were killed humanely.

5.2.11. HTT in marmoset experimental design

Drug treatments were assigned according to a blind random crossover design. One hour before the test, four to seven animals were dosed orally with vehicle or test compounds (1 ml/kg). After a washout period of at least three days, treatments were reassigned and the study was complete when all animals had received all treatments.

5.2.12. Drugs and materials for GFT and HTT test

GR73632 was dissolved in phosphate buffer solution (0.01 M) and frozen at −20 °C in 0.5 ml aliquots at the required concentration until use. Compound **3a** was prepared as a solution in methocel (0.5% in distilled water) and DMSO (5% in gerbil and 1% in marmoset). All further dilutions were performed maintaining the same ratio between water and DMSO. This vehicle was used for the treatment of the control group of animals.

5.2.13. Data analysis for GFT and HTT test

The doses of **3a** inhibiting foot tapping by 50% (ID_{50}) were determined by a linear regression analysis using RS-1 software (±C.I. 95%). Data of number of postures or jumps were subjected to a paired *t*-test, comparing each compound dose with the related vehicle treatment, using GB-stat software. Data are expressed as mean ± standard deviation.

5.2.14. Social interaction (SI) test in gerbils

The subjects were male Mongolian Gerbils (50–70 g) obtained from the Charles River colony (Germany). Animals were housed in groups of 5 under standard laboratory conditions (23 ± 1 °C; lights on 0600–1800 h). Food and water were available *ad libitum*. Testing took place in a square Perspex box (40 × 40 cm and 30 cm high) the floor of which was divided into squares (16 × 16 cm) to allow assessment of line crossings as an index of locomotor activity. Experiments were performed during the light phase between the hours of 0900 and 1300 and behavior was recorded remotely by videocamera. The day before testing, each gerbil was placed singly into the test arena and given a 10 min familiarization trial. On the day of the test, pairs of gerbils, matched for the treatment condition, but unfamiliar to each other, were placed in the centre of the test arena and their social interaction (sniffing, following, grooming the partner, wrestling) was recorded for 5 min. After each trial the floor was wiped with alcohol solution (20%) and allowed to dry prior to further testing. An observer who was blind to the drug treatment administered to the animals, analysed the tape recordings to assess the time spent in active social interaction and locomotor activity (number of line crossings).[26] Each gerbil was allocated to an unfamiliar partner that came from a different cage. Pairs of gerbils received vehicle or test compound (i.p. 2 ml/kg or p.o. 10 ml/kg) according to a randomized experimental design. Each animal was treated with compounds or vehicle one hour prior to test. No animal was tested on more than one occasion. On completion of experiments animals were humanely killed by cervical dislocation, and brains were immediately removed and frozen in isopentane at −30 °C.

5.2.15. Ex vivo receptor autoradiography

Coronal sections (12 μm thickness) of gerbil brains (3 animals/group) were used for ex vivo autoradiography experiments with the radiolabeled NK_1 receptor antagonist [^{3}H]-GR205171. To minimise the dissociation of the drug/receptor complex formed in vivo, brain sections were not washed prior to incubation with the radioligand. Total binding (0.3 nM [^{3}H]-GR205171 in Tris–HCl pH 7.4 + 3 mM $MnCl_2$, 0.02% Bovine Serum Albumin + protease inhibitors) was determined at a restricted incubation time of 10 min to minimise dissociation. The concentration of [^{3}H]-GR205171 used in this study approximates its affinity constant for the NK_1 receptor and in previous autoradiography experiments it was demonstrated to show an optimal signal/noise ratio. Non-specific binding on adjacent sections was determined in the presence of 100 nM GR205171. Following 4 × 1 min washes in the same buffer, sections were exposed to Fuji imaging plates (Fuji Photo Film, Tokyo) for 10 days. The film autoradiograms were scanned using a BAS-5000 Bio-imaging Analyzer (Fuji Photo Film, Tokyo) and quantified using an image analysis software system (AIS 4.0, Imaging Research Inc., Canada). Ex vivo binding was measured in the striatum, a brain region with high density of NK_1 binding sites, both in preclinical species[49–51] and humans, often considered a reference brain area in human PET studies.[52]

5.2.16. Drugs and materials for SI and autoradiography study

Compound **3a** was suspended in methocel (0.5% w/v in distilled water) + DMSO (5%).

Diazepam (M/890001-339, F.I.S. S.p.A.) was used as standard anxiolytic drugs and was prepared as a solution in distilled water. [^{3}H]-GR205171 (code TRQ10127, Amersham Biosciences). Specific activity: 83 Ci/mmol. Data Analysis for SI test and receptor autoradiography.

Behavioral data were subjected to one-way analysis of variance (ANOVA) followed by Dunnett's *t*-test, or a paired *t*-test comparing each compound dose with the related vehicle treatment, using GB-stat software (Version 6.5, Dynamic Microsystems Inc.).

Ex vivo [^{3}H]-GR205171 binding was expressed as the percentage of optical density versus saline treated animals. Non-specific binding on adjacent sections, determined in the presence of 100 nM GR205171, was subtracted from each total binding section to obtain the specific binding. Therefore, percentages of receptor occupancy correspond to 100% minus the percentage ratio of specific binding in the drug treated over the vehicle treated animals.

6. Molecular modeling studies

Molecular modeling studies were performed using the Molecular Operating Environment (MOE).[53] The set of NK_1 receptor antagonists selected in literature antagonists standards and compound **3a** were initially sketched in 2D and then fully minimized using the MMFF94x force field. After visual inspection the molecules were then submitted to the conformational search module, using the LowModeMD method and defaults parameters. A conformational database of 513 conformations was then used as input for the pharmacophoric elucidate module. Also in this case defaults parameters where applied. The resulting best hypothesis based on the maximum common conformation overlap index (6.98 in our case) was then used to search a molecule's **3a**, **3b** conformational database prepared using the same protocol described for the NK_1 receptor antagonists reference molecules.

Acknowledgments

This work was sponsored by G.S.K. Romano Di Fabio, Giuseppe Alvaro, Simone Braggio, Renzo Carletti, Philip A. Gerrard, Cristiana Griffante, Carla Marchioro, Alfonso Pozzan, Sergio Melotto, Alessandro Poffe, Laura Piccoli, Emiliangelo Ratti, Elvira Tranquillini, Michael Trower, Simone Spada, Mauro Corsi were employees of GSK (Neurosciences Centre of Excellence for Drug Discovery, Medicines Research Centre, Via A. Fleming 4, 37135 Verona, Italy) at the time this work was performed. Emiliangelo Ratti and Michael Trower are currently employees and shareholders in NeRRe Therapeutics Ltd, which owns the intellectual property and development rights to **3a** (also called orvepitant).

References and notes

1. Harrison, S.; Geppetti, P. *Int. J. Biochem. Cell B* **2001**, *33*, 555.
2. Zhongli, G.; Peet, N. P. *Curr. Med. Chem.* **1999**, *6*, 375.
3. Satake, H.; Kawada, T. *Curr. Drug Targets* **2006**, *7*, 963.
4. Chahl, L. A. *Curr. Drug Targets* **2006**, *7*, 993.
5. Ebner, K.; Singewald, N. *Amino Acids* **2006**, *31*, 251.
6. McLean, S. *Curr. Pharm. Des.* **2005**, *11*, 1529.
7. Nemeroff, C. B. *Psychopharmacol. Bull.* **2002**, *36*, 6.
8. Mantyh, P. W. *J. Clin. Psychiatry* **2002**, *63*, 6.
9. Wong, M. L.; Licinio, J. *Nat. Rev. Drug Disc.* **2004**, *3*, 136.
10. Holtzheimer, P. E.; Nemeroff, C. B. *Novel Curr. Pshychiatry Rep.* **2008**, *10*, 465.
11. Patacchini, R.; Maggi, C. A. *Eur. J. Pharmacol.* **2001**, *429*, 13.
12. Rupniak, N. M.; Kramer, M. S. *TiPS* **1999**, *20*, 485.
13. Muñoz, M.; Coveñas, R. *Curr. Med. Chem.* **2011**, *18*, 1820.
14. Kramer, M. S.; Cutler, N.; Feighner, J.; Shrivastava, R.; Carman, J.; Sramek, J. J.; Reines, S. A.; Liu, G.; Snavely, D.; Wyatt-Knowles, E.; Hale, J. J.; Mills, S. G.; MacCoss, M.; Swain, C. J.; Harrison, T.; Hill, R. G.; Hefti, F.; Scolnick, E. M.; Cascieri, M. A.; Chicchi, G. G.; Sadowski, S.; Williams, A. R.; Hewson, L.; Smith, D.; Carlson, E. J.; Hargreaves, R. J.; Rupniak, N. M. J. *Science* **1998**, *281*, 1640.
15. Czéh, B.; Fuchs, E.; Simon, M. *Expert Opin. Investig. Drugs* **2006**, *15*, 479.

16. Kramer, M. S.; Winokur, A.; Kelsey, J.; Preskorn, S. H.; Rothschild, A. J.; Snavely, D.; Ghosh, K.; Ball, W. A.; Reines, S. A.; Munjack, D.; Apter, J. T.; Cunningham, L.; Kling, M.; Bari, M.; Getson, A.; Lee, Y. *Neuropsychopharmacology* **2004**, *29*, 385.
17. Chappell, P.B. 11th Congress of the Association of, European Psychiatry, 2002.
18. Keller, M.; Montgomery, S.; Ball, W.; Morrison, M.; Snavely, D.; Liu, G.; Hargreaves, R.; Hietala, J.; Lines, C.; Beebe, K.; Reines, S. *Biol. Psychia.* **2006**, *59*, 216.
19. Ratti, E.; Bellew, K.; Bettica, P.; Bryson, H.; Zamuner, S.; Archer, G.; Squassante, L.; Bye, A.; Trist, D. G.; Krishnan, K. R.; Fernandes, S. *J. Clin. Psychopharmacol.* **2011**, *31*, 727.
20. Di Fabio, R.; Alvaro, G.; Griffante, C.; Pizzi, D. A.; Donati, D.; Mattioli, M.; Cimarosti, D.; Guercio, G.; Marchioro, C.; Provera, S.; Zonzini, L.; Montanari, D.; Melotto, S.; Gerrard, P. A.; Trist, D. G.; Ratti, E.; Corsi, M. *J. Med. Chem.* **2011**, *54*, 1071.
21. Manetti, D.; Gherlandini, C.; Bartolini, A.; Bellucci, C.; Dei, S.; Galeotti, N.; Gualtieri, F.; Romanelli, M. N.; Scapecchi, S.; Teodori, E. *J. Med. Chem.* **2000**, *43*, 1969.
22. Piwinski, J. J.; Wong, J. K.; Green, M. J.; Kaminski, J. J.; Colizzo, F.; Albanese, M. M.; Ganguly, A. K.; Billah, M. M.; Anthes, J. C.; West, R. E., Jr. *Bioorg. Med. Chem. Lett.* **1998**, *8*, 3469.
23. The absolute stereochemistry of intermediates 1a and 1b was assigned by X-ray studies; see Alvaro, G.; Di Fabio, R.; Tranquillini, E.; Spada, S. Piperidine Derivatives, WO2003066635.
24. Pellegatti, M.; Bordini, E.; Fizzotti, P.; Roberts, A.; Johnson, B. M. *Drug Met. Dispos.* **2009**, *37*, 1635.
25. Ferrari, L.; Reami, D.; Michi, M. *J. Chromatogr. B* **2010**, *878*, 2974.
26. Miraglia, L.; Pasciarusco, S.; Bordini, E.; Martinucci, S.; Pellegatti, M. *Drug Met. Dispos.* **2010**, *38*, 1876.
27. Griffante, C.; Carletti, R.; Andretta, F.; Corsi, M. *Br. J. Pharmacol.* **2006**, *148*, 39.
28. Di Fabio, R.; Alvaro, G.; Griffante, C.; Pentassuglia, G.; Pizzi, D. A.; Donati, D.; Rossi, T.; Guercio, G.; Mattioli, M.; Cimarosti, Z.; Marchioro, C.; Provera, S.; Zonzini, L.; Montanari, D.; Melotto, S.; Gerrard, P. A.; Trist, D. G.; Ratti, E.; Corsi, M. *J. Med. Chem.* **2009**, *52*, 3238.
29. Ballard, T. M.; Breitmaier, E.; Grottick, A. J.; Koch, S.; Higgins, G. A. *Behav. Pharmacol.* **1999**, *10*, S5.
30. Rupniak, N. M. J.; Williams, A. R. *Eur. J. Pharmacol.* **1994**, *265*, 179.
31. Steckler, T. *Curr. Top. Behav. Neurosci.* **2010**, *2*, 415.
32. Costall, B.; Domeney, A. M.; Gerrard, P. A.; Naylor, R. J. *Br. J. Pharmacol.* **1988**, *95*, 475P.
33. Lipp, H. P. *Brain Behav. Biol.* **1978**, *15*, 241.
34. Cheeta, S.; Tucci, S.; Sandhu, J.; Williams, A. R.; Rupniak, N. M. J.; File, S. E. *Brain Res.* **2001**, *915*, 170.
35. Beresford, I. J.; Birch, P. J.; Hagan, R. M.; Ireland, S. J. *Br. J. Pharmacol.* **1991**, *104*, 292.
36. Langlois, X.; Riele, P. T.; Wintmolders, C.; Leysen, J. E.; Jurzak, M. *J. Pharmacol. Exp. Ther.* **2001**, *299*, 712.
37. Seabrook, G. R.; Shepheard, S. L.; Williamson, D. J.; Tyrer, P.; Rigby, M.; Cascieri, M. A.; Harrison, T.; Hargreaves, R. J.; Hill, R. G. *Eur. J. Pharm.* **1996**, *317*, 129.
38. Beattie, D. T.; Beresford, J. M.; Connor, H. E.; Marshall, F. H.; Hawcock, A. B.; Hagan, R. M.; Bowers, J.; Birch, P. J.; Ward, T. P. *Br. J. Pharmacol.* **1995**, *116*, 3149.
39. Hoffmann, T.; Bös, M.; Stadler, H.; Schnider, P.; Hunkeler, W.; Godel, T.; Galley, G.; Ballard, T. M.; Higgins, G. A.; Poli, S. M.; Sleight, A. J. *Bioorg. Med. Chem. Lett.* **2006**, *16*, 1362.
40. Elliott, J. M.; Carlson, E. J.; Chicchi, G. G.; Dirat, O.; Dominguez, M.; Gerhard, U.; Jelley, R.; Jones, A. B.; Kurtz, M. M.; Lan Tsao, K.; Wheeldon, A. *Bioorg. Med. Chem. Lett.* **2006**, *16*, 2929.
41. Jacoby, E.; Boudon, A.; Kucharczyk, N.; Michel, A.; Fauchere, J. L. *J. Recept. Signal Transduction Res.* **1997**, *17*, 855.
42. Takeuchi, Y.; Shands, E. F.; Beusen, D. D.; Marshall, G. R. *J. Med. Chem.* **1998**, *41*, 3609.
43. Caliendo, G.; Grieco, P.; Perissutti, E.; Santagada, V.; Saviano, G.; Tancredi, T.; Temussi, P. A. *J. Med. Chem.* **1997**, *40*, 594.
44. Ratti, E.; Bettica, P.; Alexander, R.; Archer, G.; Carpenter, D.; Evoniuk, G.; Gomeni, R.; Lawson, E.; Lopez, M.; Millns, H.; Rabiner, E. A.; Trist, D.; Trower, M.; Zamuner, S.; Krishnan, R.; Fava, M. *J Psychopharmacol.* **2013**, *27*, 424.
45. Lundstrom, K.; Hawcock, A. B.; Vargas, A.; Ward, P.; Thomas, P. Z.; Naylor, A. *Eur. J. Pharmacol.* **1997**, *337*, 73.
46. Beattie, D. T.; Beresford, I. J.; Connor, H. E.; Marshall, F. H.; Hawcock, A. B.; Hagan, R. M.; Bowers, J.; Birch, P. J.; Ward, P. *Br. J. Pharmacol.* **1995**, *116*, 3149.
47. Cheng, Y.; Prusoff, W. H. *Biochem. Pharmacol.* **1973**, *22*, 3099.
48. Munson, P. J.; Rodbard, D. *Anal. Biochem.* **1980**, *107*, 220.
49. Saffroy, M.; Beaujouan, J. C.; Torrens, Y.; Besseyre, J.; Bergstrom, L.; Glowinski, J. *Peptides* **1988**, *9*, 227.
50. Dam, T. V.; Quirion, R. *Peptides* **1986**, *7*, 855.
51. Caberlotto, L.; Hurd, Y. L.; Murdock, P.; Wahlin, J. P.; Melotto, S.; Corsi, M.; Carletti, R. *Eur. J. Neurosci.* **2003**, *17*, 1736.
52. Hargreaves, R. *J. Clin. Psychiatry* **2002**, *63*, 18.
53. Molecular Operating Environment (MOE), 2012.10; Chemical Computing Group Inc., 1010 Sheerbrooke St. West, Suite #910, Montral, QC, Canada, H3A 2R7, 2012.